

Detecting coherent transport structures in ocean surface flows

Leah Hoogstra

Advisor: Dr. Paul Choboter

Project Leader: Dr. Ryan Walter

June 13, 2023

Introduction

- Fluid dynamics are rooted in chaos, yet familiar structures emerge time and again
- Lagrangian coherent structures (LCS) describe some of these patterns, breaking up the flow into its most influential parts
- LCSs are the "skeleton" of a fluid flow

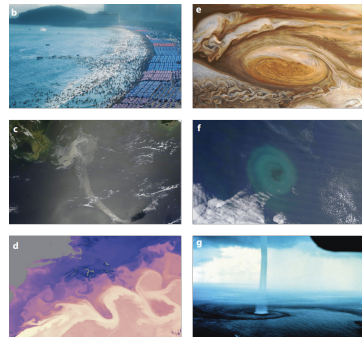


Figure: Examples of coherent patterns found in nature [3]

What is an LCS?

- “Coherent structure”: a surface within the flow that maintains its character over time
- “Lagrangian”: they move with the flow
 - Lagrangian vs. Eulerian perspective
- LCSs are transport barriers
- LCSs have the locally strongest influence on the fluid around them



Figure: The boundary of a tornado is a good visual example of an LCS

What is an LCS?

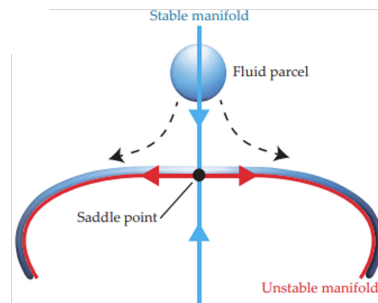


Tornado example: the outer edge of a tornado is an LCS

- Made up of air, but has properties distinct from the air around it
- Maintains its shape and characteristics as it moves through the air
- Locally most influential structure
- Transport barrier
- Exists for a finite amount of time

Hyperbolic LCSs: Saddle Point Analogy

Hyperbolic LCSs are analogs of a classic saddle point in a dynamical system



Stable manifold → repelling LCS
Unstable manifold → attracting LCS

How do we detect LCSs?

- Multiple proposed mathematical definitions
- Focus: two proposed by Dr. George Haller
 - ① Finite-time Lyapunov exponents (FTLEs)
 - ② Geodesic detection
- Haller argues geodesic detection is the better definition, but most researchers still use FTLEs.
Why?



Terminology

We introduce the following notation describing a 2-D fluid flow

$$\mathbf{x} = [x, y]$$

position vector

$$\mathbf{v} = [u, v]$$

velocity vector

with the relationship

$$\dot{\mathbf{x}} = \frac{d\mathbf{x}}{dt} = \mathbf{v}(\mathbf{x}, t)$$

and conditions

$$\mathbf{x} \in U \subset \mathbb{R}^2$$

bounded domain

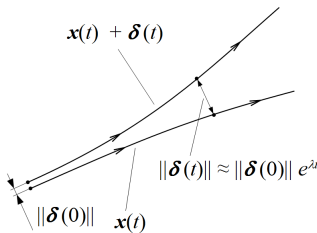
$$t \in [\alpha, \beta] \subset \mathbb{R}$$

finite time

Lyapunov Exponents

The Lyapunov exponent λ measures trajectory separation after perturbation of initial conditions

$$\|\delta \mathbf{x}(t)\| \approx \|\delta \mathbf{x}_0\| e^{\lambda t}$$



The maximal Lyapunov exponent (MLE) dominates as $t \rightarrow \infty$

Finite Time Lyapunov Exponents

FTLEs adapt MLEs to finite-time systems.

- Let $[t_0, t]$ be the time window of interest where $t = t_0 + T$.
- The **flow map** $F_{t_0}^t(x_0)$ maps an initial position x_0 to its position at time t .

$$F_{t_0}^t(x_0) = x_0 + \int_{t_0}^{t_0+T} v(x(\tau), \tau) d\tau.$$

Finite Time Lyapunov Exponents

Two key quantities capture deformation of a fluid parcel:

- The **deformation gradient** $\nabla \mathbf{F}_{t_0}^t(x_0)$

$$\nabla \mathbf{F}_{t_0}^t = \begin{pmatrix} \frac{\partial x}{\partial x_0} & \frac{\partial y}{\partial x_0} \\ \frac{\partial x}{\partial y_0} & \frac{\partial y}{\partial y_0} \end{pmatrix}$$

- The **Cauchy-Green strain tensor** $\mathbf{C}_{t_0}^t(x_0)$

$$\mathbf{C}_{t_0}^t(x_0) = [\nabla \mathbf{F}_{t_0}^t(x_0)]^* \nabla \mathbf{F}_{t_0}^t(x_0)$$

where * is the matrix transpose.

Finite Time Lyapunov Exponents

- The eigenvectors of $\mathbf{C}_{t_0}^t(\mathbf{x}_0)$ give the directions of most stretching and shrinking

$$0 < \lambda_1 \leq \dots \leq \lambda_n \quad |\xi_i| = 1$$

- FTLE Definition:

$$\Lambda_{t_0}^t(\mathbf{x}_0) = \frac{1}{|t - t_0|} \log \left(\sqrt{\lambda_n(t, t_0, \mathbf{x}_0)} \right)$$

- LCSs are ridges of the FTLE field

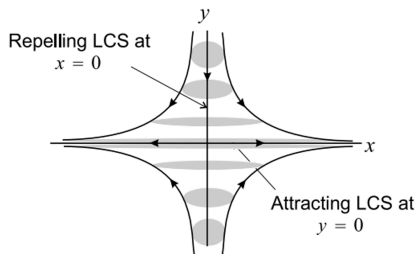
FTLE Example

$$\dot{x} = \tanh(x)$$

$$\dot{y} = -y$$

FTLE Example

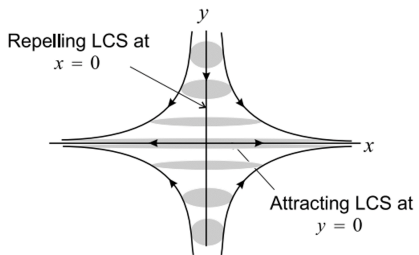
$$\begin{aligned}\dot{x} &= \tanh(x) \\ \dot{y} &= -y\end{aligned}$$



FTLE Example

$$\begin{aligned}\dot{x} &= \tanh(x) \\ \dot{y} &= -y\end{aligned}$$

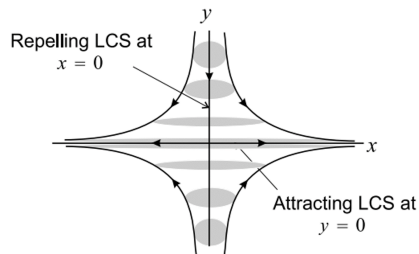
$$C_{t_0}(x_0) = \begin{pmatrix} \frac{e^{2T} \cosh^2(x_0)}{1+e^{2T} \sinh^2(x_0)} & 0 \\ 0 & e^{-2T} \end{pmatrix}$$



FTLE Example

$$\begin{aligned}\dot{x} &= \tanh(x) \\ \dot{y} &= -y\end{aligned}$$

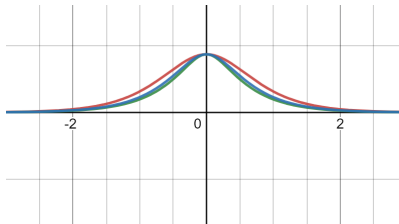
$$C_{t_0}^t(x_0) = \begin{pmatrix} \frac{e^{2T} \cosh^2(x_0)}{1 + e^{2T} \sinh^2(x_0)} & 0 \\ 0 & e^{-2T} \end{pmatrix}$$



$$\lambda_2(t, t_0, x_0) = \frac{e^{2T} \cosh^2(x_0)}{1 + e^{2T} \sinh^2(x_0)}, \quad \xi_2 = [1, 0]$$

FTLE Example

$$\begin{aligned}\Lambda_{t_0}^t(x_0) &= \frac{1}{|t - t_0|} \log(\sqrt{\lambda_2(t, t_0, x_0)}) \\ &= \frac{1}{|T|} \log \left(\sqrt{\frac{e^{2T} \cosh^2(x_0)}{1 + e^{2T} \sinh^2(x_0)}} \right)\end{aligned}$$

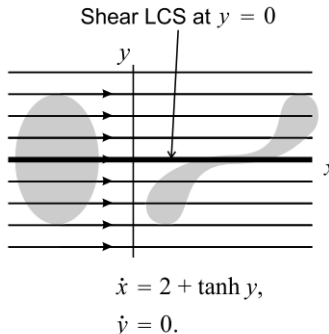


Red: $T = 0.25$, Blue: $T = 0.75$, Green: $T = 1$

Maximized at $x = 0$ for $T > 0 \implies x = 0$ is a repelling LCS.

Issues with FTLE-Defined LCSs

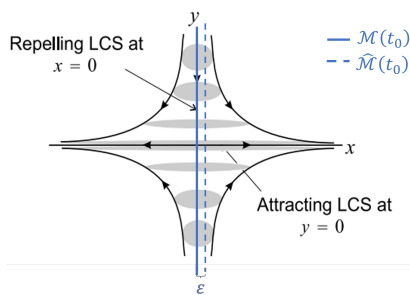
FTLE-defined LCSs can be imprecise: false positives and false negatives are an issue, not always transport barriers



FTLE method identifies the line of particle separation, but it is not due to a repelling LCS

Geodesics

- FTLEs measure separation and then find curves.
- Geodesic LCSs start with curves and measure their effects on nearby particles.
- Considers material surfaces $\mathcal{M}(t)$, time-constant slices of an invariant manifold
- Checks if $\mathcal{M}(t)$ is a locally strongest repelling or attracting surface
- Name comes from the algorithm for finding them



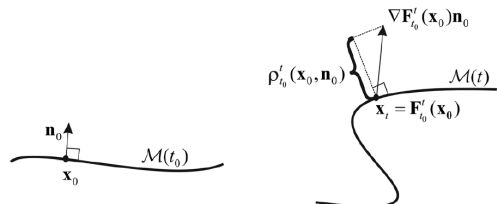
Geodesics

Let \mathbf{n}_t be the vector normal to the position \mathbf{x}_t at time t .

Under the flow map

$\nabla \mathbf{F}_{t_0}^t(\mathbf{x}_0)$:

- $\mathbf{x}_0 \rightarrow \mathbf{x}_t$
- $\mathbf{n}_0 \rightarrow \nabla \mathbf{F}_{t_0}^t(\mathbf{x}_0) \mathbf{n}_0$
- $\mathbf{e}_0 \rightarrow$
 $\nabla \mathbf{F}_{t_0}^t(\mathbf{x}_0) \mathbf{e}_0 = c \mathbf{e}_t$ for
some $c \in \mathbb{R}$



We project the advected normal vector onto the new normal vector \mathbf{n}_t to measure its growth or decay.

$$\rho_{t_0}^t(\mathbf{x}_0, \mathbf{n}_0) = \langle \mathbf{n}_t, \nabla \mathbf{F}_{t_0}^t(\mathbf{x}_0) \mathbf{n}_0 \rangle$$

Geodesics: Repulsion Rate and Repulsion Ratio

- Repulsion rate measures growth or decay of normal vector \mathbf{n}_0 after advection

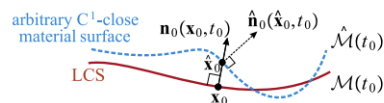
$$\rho_{t_0}^t(\mathbf{x}_0, \mathbf{n}_0) = \langle \mathbf{n}_t, \nabla \mathcal{F}_{t_0}^t(\mathbf{x}_0) \mathbf{n}_0 \rangle$$

- Repulsion ratio measures this growth in comparison to growth of tangent vector \mathbf{e}_0

$$\nu_{t_0}^t = \min_{\mathbf{e}_0 \in \mathcal{T}_{x_0}} \frac{\rho_{t_0}^t(\mathbf{x}_0, \mathbf{n}_0)}{|\mathbf{e}_t|}$$

If both $\rho > 1$ and $\nu > 1$, $\mathcal{M}(t)$ is a repelling material surface.

Repelling LCSs have locally maximal ρ values.



$$\rho_{t_0}^{t_0+T}(\hat{\mathbf{x}}_0, \hat{\mathbf{n}}_0) < \rho_{t_0}^{t_0+T}(\mathbf{x}_0, \mathbf{n}_0)$$

Relationship to CG Tensor

Repulsion rate and repulsion ratio can be calculated using the Cauchy-Green strain tensor

$$\rho_{t_0}^t(\mathbf{x}_0, \mathbf{n}_0) = \frac{1}{\sqrt{\langle \mathbf{n}_0, [\mathbf{C}_{t_0}^t(\mathbf{x}_0)]^{-1} \mathbf{n}_0 \rangle}}$$

$$\nu_{t_0}^t(\mathbf{x}_0, \mathbf{n}_0) = \min_{\mathbf{e}_0 \in T_{x_0}} \frac{\rho_{t_0}^t(\mathbf{x}_0, \mathbf{n}_0)}{\langle \mathbf{e}_0, \mathbf{C}_{t_0}^t(\mathbf{x}_0) \mathbf{e}_0 \rangle}$$

Geodesic method uses eigenvectors of $\mathbf{C}_{t_0}^t(\mathbf{x}_0)$, $\nabla \lambda_n(t, t_0, \mathbf{x}_0)$, and $\nabla^2 \lambda_n(t, t_0, \mathbf{x}_0)$ to identify curves $\mathcal{M}(t)$ with maximal values of ρ

Geodesics: Conditions for a Repelling LCS

Theorem (Haller 2011, Sufficient and Necessary Conditions for LCS in Two Dimensions [2])

Consider a compact material line $\mathcal{M}(t) \subset U$ over the interval $[t_0, t_0 + T]$. Then $\mathcal{M}(t)$ is a repelling Weak LCS if and only if the following hold for all $x_0 \in \mathcal{M}(t_0)$:

- ① $\lambda_1(x_0, t_0, T) \neq \lambda_2(x_0, t_0, T) > 1$;
- ② $\xi_2(x_0, t_0, T) \perp T_{x_0}\mathcal{M}(t_0)$;
- ③ $\langle \nabla \lambda_2(x_0, t_0, T), \xi_2(x_0, t_0, T) \rangle = 0$;

where $T_{x_0}\mathcal{M}(t_0)$ is the space tangent to $\mathcal{M}(t_0)$ at the point x_0 . $\mathcal{M}(t)$ is a **repelling LCS** if and only if $\mathcal{M}(t)$ satisfies the above conditions and the following condition for all $x_0 \in \mathcal{M}(t_0)$:

- ④ $\langle \xi_2, \nabla^2 \lambda_2 \xi_2 \rangle < 0$

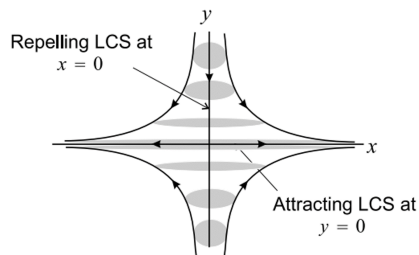
Geodesics Example

Same system as in FTLE example:

$$\dot{x} = \tanh(x)$$

$$\dot{y} = -y$$

$$C_{t_0}^t(x_0) = \begin{pmatrix} \frac{e^{2T} \cosh^2(x_0)}{1+e^{2T} \sinh^2(x_0)} & 0 \\ 0 & e^{-2T} \end{pmatrix}$$



$$\lambda_2(t, t_0, x_0) = \frac{e^{2T} \cosh^2(x_0)}{1 + e^{2T} \sinh^2(x_0)}, \quad \xi_2 = [1, 0]$$

Geodesics Example

$$\lambda_2(t, t_0, x_0) = \frac{e^{2T} \cosh^2(x_0)}{1 + e^{2T} \sinh^2(x_0)}, \quad \text{Forward time} \implies T > 0$$

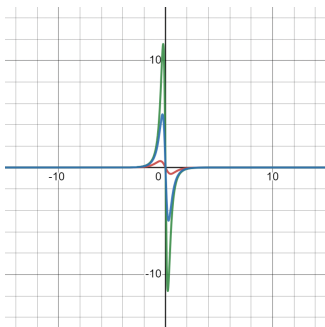


Figure: $\nabla\lambda_2$ has a zero at $x = 0$

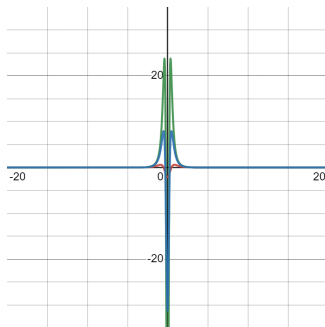


Figure: $\nabla^2\lambda_2$ is negative at $x = 0$

Technique Comparison

FTLE Definition

Geodesic Definition

Technique Comparison

FTLE Definition

- Simple, easy to implement, identifies 2 of 3 LCS types

Geodesic Definition

- Complex, requires many parameters set up front, identifies all 3 LCS types

Technique Comparison

FTLE Definition

- Simple, easy to implement, identifies 2 of 3 LCS types
- Can be imprecise, does not account for direction of flow near the LCS

Geodesic Definition

- Complex, requires many parameters set up front, identifies all 3 LCS types
- Precise, errs on the side of being too strict

Technique Comparison

FTLE Definition

- Simple, easy to implement, identifies 2 of 3 LCS types
- Can be imprecise, does not account for direction of flow near the LCS
- Not all LCSs identified are transport barriers

Geodesic Definition

- Complex, requires many parameters set up front, identifies all 3 LCS types
- Precise, errs on the side of being too strict
- All LCSs identified are transport barriers

Technique Comparison

FTLE Definition

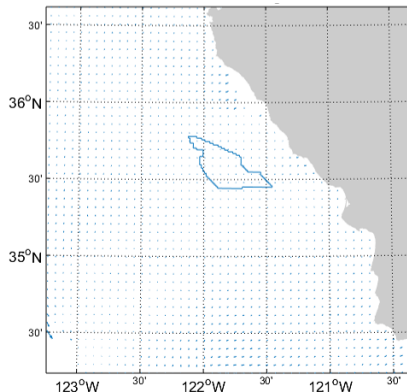
- Simple, easy to implement, identifies 2 of 3 LCS types
- Can be imprecise, does not account for direction of flow near the LCS
- Not all LCSs identified are transport barriers
- Not a good method for high stakes transport problems (e.g. oil spills, search and rescue), but likely okay for statistical studies

Geodesic Definition

- Complex, requires many parameters set up front, identifies all 3 LCS types
- Precise, errs on the side of being too strict
- All LCSs identified are transport barriers
- Works well for statistical studies or higher stakes applications, though tools need improvement for wider audience

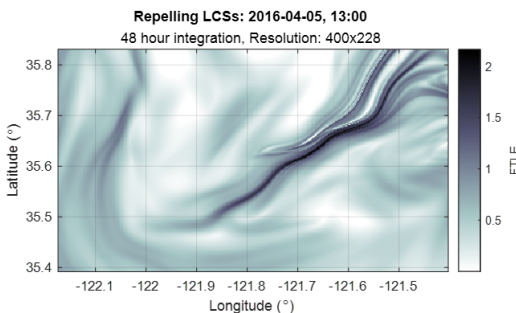
Application: Morro Bay Wind Energy Area

- Dec 2022 BOEM lease sale for offshore wind development
- Need to characterize currents and transport processes
- MB WEA: about 20 miles offshore, 376 sq. miles
- Obtained surface current history from CenCOOS' high-frequency radar data, 2012-2021, 6km resolution



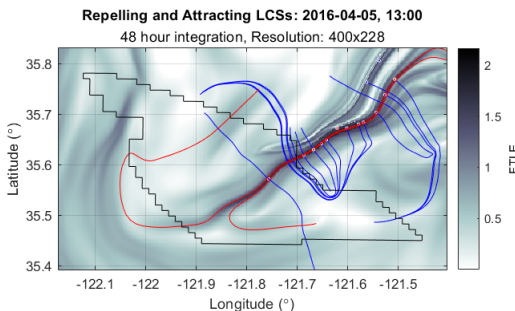
Grid of HFR velocity data with WEA outlined

WEA Application



LCSs identified in the WEA, April 5-7, 2016. Forward FTLE field is shaded.

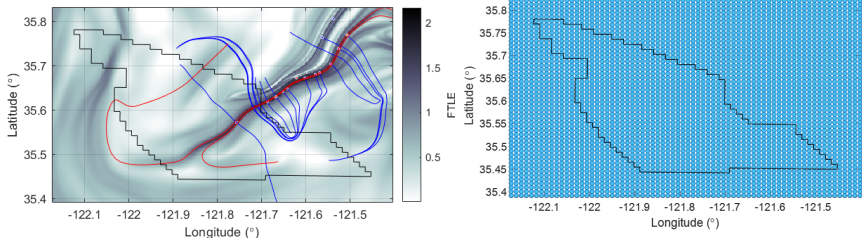
WEA Application



LCSs identified in the WEA, April 5-7, 2016. Forward FTLE field is shaded. Geodesic repelling LCSs are outlined in red, geodesic attracting LCSs in blue.

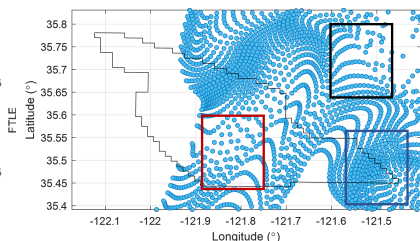
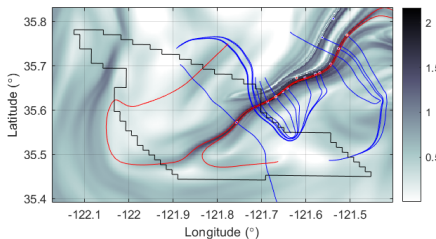
WEA Application

Compare to results of flow map



WEA Application

We see clear markers of repelling LCS, attracting LCS, saddle point

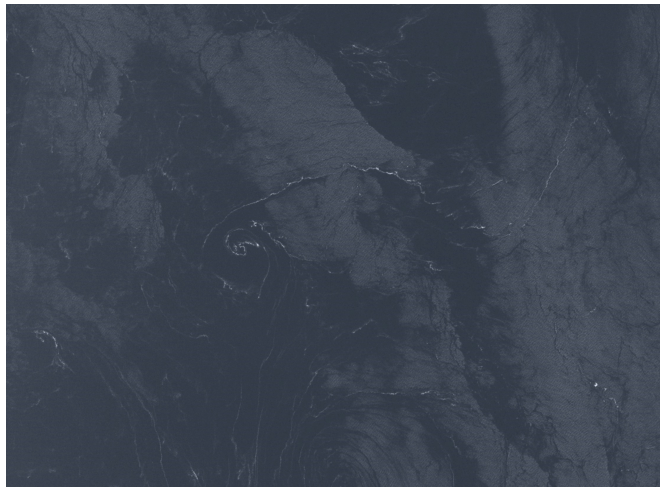


Velella velella Application

- Thousands of by-the-wind sailors (*velella velella*) have washed up on California beaches this spring
- Since these creatures float with the currents, they gather along attracting LCSs.



Velella velella Application



Velella velella spiral seen on May 6th, 2023

Velella velella Application

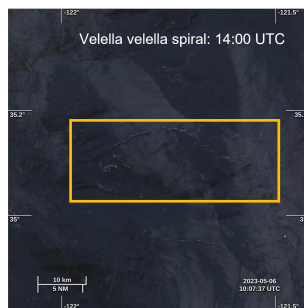
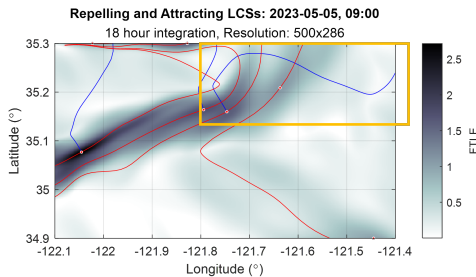


Figure: Attracting LCS in shape of velella spiral, 11 hours before satellite snapshot

Conclusions

- The best LCS method can depend on the application
- Methods may be best used in combination. FTLEs as a first look, eigenvector field and/or geodesics for more detail and precision
- Future work for LCS research:
 - Quantify rate of misidentification for FTLEs, further develop best practices
 - Accessible software development incorporating best practices
- Future work for WEA research:
 - Further analyze robustness of results
 - Identify LCS patterns in the region over time
 - Explore other LCS definitions, esp. clustering techniques

References

- [1] Alireza Hadjighasem et al. "A critical comparison of Lagrangian methods for coherent structure detection". In: *Chaos: An Interdisciplinary Journal of Nonlinear Science* 27.5 (2017), p. 053104.
- [2] George Haller. "A variational theory of hyperbolic Lagrangian coherent structures". In: *Physica D: Nonlinear Phenomena* 240.7 (2011), pp. 574–598.
- [3] George Haller. "Lagrangian coherent structures". In: *Annual review of fluid mechanics* 47 (2015), pp. 137–162.
- [4] Saviz Mowlavi et al. "Detecting Lagrangian coherent structures from sparse and noisy trajectory data". In: *Journal of Fluid Mechanics* 948 (2022), A4.
- [5] Kristjan Onu, Florian Huhn, and George Haller. "LCS Tool: A computational platform for Lagrangian coherent structures". In: *Journal of Computational Science* 7 (2015), pp. 26–36.

Types of LCSs

LCSs are usually categorized as hyperbolic, elliptic, or parabolic

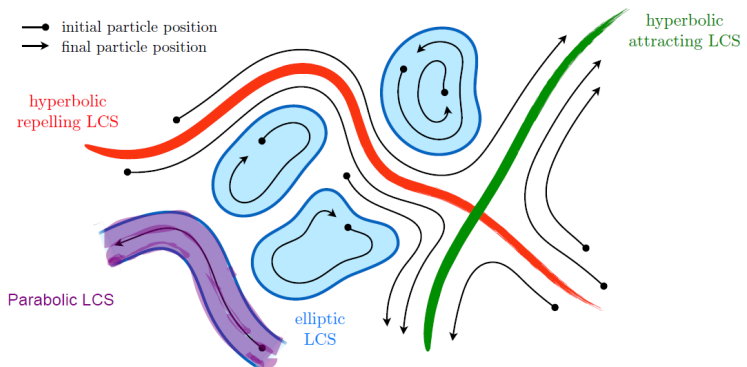


Figure: Behavior of the three main types of LCSs [4]

Proof that $\mathbf{e}_t \in \mathcal{T}_{\mathbf{x}_0} \mathcal{M}(t_0)$

Proof the Advected Tangent Vector Remains Tangent

$$0 = \langle \mathbf{e}_0, \mathbf{n}_0 \rangle$$

$$= \langle \mathbf{e}_0, (\nabla \mathbf{F}_t^{t_0} \nabla \mathbf{F}_{t_0}^t)^* \mathbf{n}_0 \rangle$$

$$= \langle \mathbf{e}_0, (\nabla \mathbf{F}_{t_0}^t)^* (\nabla \mathbf{F}_t^{t_0})^* \mathbf{n}_0 \rangle$$

$$= \langle \nabla \mathbf{F}_{t_0}^t \mathbf{e}_0, (\nabla \mathbf{F}_t^{t_0})^* \mathbf{n}_0 \rangle$$

$$= \langle \nabla \mathbf{F}_{t_0}^t \mathbf{e}_0, \mathbf{n}_t \rangle$$

Repulsion Rate's Connection to CG Tensor

$$\begin{aligned}\rho_{t_0}^t(x_0, n_0) &= \langle n_t, \nabla F_{t_0}^t(x_0) n_0 \rangle \\&= \left\langle \frac{\nabla F_t^{t_0}(x_t)^* n_0}{|\nabla F_t^{t_0}(x_t)^* n_0|}, \nabla F_{t_0}^t(x_0) n_0 \right\rangle \\&= \frac{\langle n_0, \nabla F_t^{t_0}(x_t) \nabla F_{t_0}^t(x_0) n_0 \rangle}{\sqrt{\langle n_0, (\nabla F_t^{t_0}) (\nabla F_t^{t_0})^* n_0 \rangle}} \\&= \frac{1}{\sqrt{\langle n_0, [C_{t_0}^t(x_0)]^{-1} n_0 \rangle}}\end{aligned}$$

Cauchy-Green Strain Tensor Origin

Polar decomposition theorem: $\mathbf{F}_{t_0}^t = RU$

- R orthogonal, describes rotations
- U symmetric and positive definite, describes extensions
- $\mathbf{C}_{t_0}^t = U^2 = F^T F$

Geodesic Algorithm Notes

2.2 Hyperbolic LCSs

Next we consider positions of material lines at time t_0 that prevail as most repelling or attracting material lines (or *hyperbolic LCSs*) over a time interval $[t_0, t] \subset [t_-, t_+]$. Farazmand et al. [12] argue that hyperbolic LCSs are stationary curves of the averaged shear functional

$$Q(\gamma) = \frac{1}{\sigma} \int_0^\sigma \frac{\langle r'(s), D_{t_0}^t(r(s))r'(s) \rangle}{\sqrt{\langle r'(s), C_{t_0}^t(r(s))r'(s) \rangle \langle r'(s), r'(s) \rangle}} ds, \quad D_{t_0}^t = \frac{1}{2}[C_{t_0}^t \Omega - \Omega C_{t_0}^t],$$

obtained by averaging the Lagrangian shear arising over $[t_0, t]$ along closed material lines parametrized as $r(s)$ with $s \in [0, \sigma]$. More precisely, hyperbolic LCSs are stationary curves of $Q(\gamma)$ with respect to fixed-endpoint perturbations. We note that parabolic LCSs (Lagrangian jet cores) are also stationary curves of $Q(\gamma)$, but under variable endpoint perturbations (cf. [12]).

Solutions to this variational problem turn out to be orbits of the ξ_1 or ξ_2 eigenvector field. Repelling LCSs (*shrinklines*) are obtained as trajectories of the differential equation

$$r' = \xi_1(r), \tag{6}$$

and attracting LCSs (*stretchlines*) are obtained as trajectories of the differential equation

$$r' = \xi_2(r). \tag{7}$$

Shrinklines and stretchlines coincide with the null-geodesics of the Lorentzian metric $h(u, v) = \langle u, D_{t_0}^t(r)v \rangle$. For this reason, we refer to the computation of hyperbolic LCSs as strongest normally-repelling or normally-attracting orbits of (5) as *geodesic detection of hyperbolic LCSs*.

Figure: Algorithm to find geodesic LCSs [5]

Technique Comparison

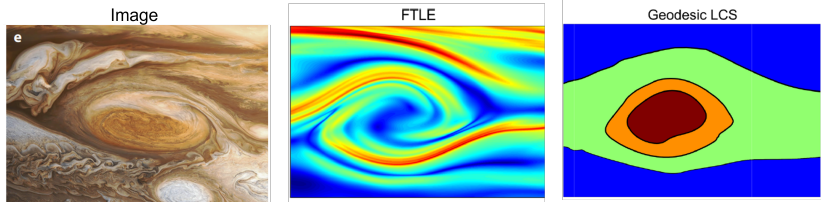
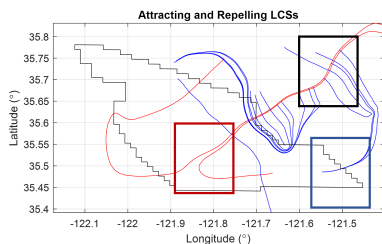
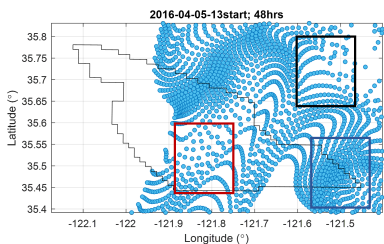
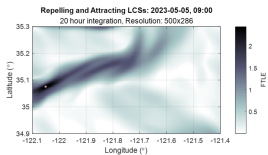
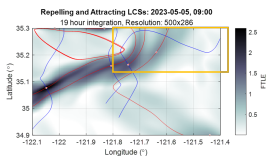
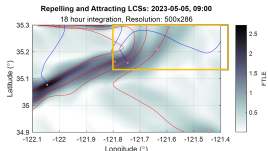


Figure: FTLE and Geodesic Detection on Jupiter wind fields near the Great Red Spot [1], [3]

Side by Side: WEA LCSs and Flow End State



Velella velella LCSs over time



Velella velella animation

Animating the flow adds to the evidence that the spiral drifted south from its formation to the time of the snapshot

